

SUPPLEMENTARY INFORMATION: PERVASIVE AEOLIAN ACTIVITY ALONG ROVER CURIOSITY'S TRAVERSE IN GALE CRATER, MARS

S.Silvestro, D.A. Vaz, R.C. Ewing, A.P. Rossi, L.K. Fenton, T.M. Michaels, J. Flahaut and P.E. Geissler

Aeolian change detection

Changes in the dune and ripple pattern were measured over three HiRISE images (0.25 meters per pixel). The images were processed in a cylindrical projection on the Mars IAU spheroid using the United States Geological Survey-ISIS (Integrated Software for Imagers and Spectrometers) software. Tracking changes in the ripple pattern and measuring the crestline displacement is challenging due to the difference in the acquisition parameters between the overlapping images. When images are taken off-nadir (i.e. with an emission angle different than 0°), geometric distortions (parallax) arise and the images may not align well. For this reason ripple migrations have only been calculated over two orthorectified images (the T1-T2 pair). The process of orthorectification over a digital terrain model (DTM) remove the parallax distortion for topographic features resolved by the DTM (> 1 m/pixel) and the image co-registration could be performed in ArcGIS with minimal error (RMS = 0.00104 and 0.068 for the pairs T1-T2 and T1-T3 respectively). The orthorectified images are freely available from the HiRISE web site (<http://hirise.lpl.arizona.edu/dtm/>). However, because the study ripple are barely resolved by the DTM, the parallax is not completely removed and our measurements suffer from an error that we are not able to quantify. Radiometric distortions arise from difference in lighting geometry. Big offsets in the sub solar azimuth (the direction of the sun) will change the direction of the shadow. In the pair T1-T2 this change is minimal (less than 8°), and for both images the light comes from the NW (top right). Differences in the season (solar longitude, Ls) cause a divergence in the solar incidence angle (the angle the sun makes with the surface relative to zenith). This causes albedo and contrast variations between the two images. This issue can be minimized in ArcGIS (brightness and contrast of one image has been adjusted to make it as similar as possible to the other).

The Mars Regional Atmospheric Modeling System (MRAMS)

The Mars Regional Atmospheric Modeling System (MRAMS first described in Rafkin et al. 2001, with further updates in Michaels and Rafkin, 2008) is a non hydrostatic, fully compressible, limited domain (i.e., not global) atmospheric model that uses nested grids to estimate/predict atmospheric conditions on Mars at high resolution. MRAMS includes cloud microphysics options, topographic shadowing and slope effects, dust entrainment/sedimentation capabilities, a state-of-the-art radiative transfer scheme for Mars, boundary layer turbulence parameterizations, surface characteristics and topography from gridded spacecraft datasets, and a multi-level subsurface thermal model. Further relevant model details and explanations are provided in the following paragraphs.

The model permits the simulation of atmospheric flows with large vertical accelerations, believed to be a relatively common occurrence on Mars. In addition it is easily configured over a wide range of user-specified regions and horizontal grid spacings (can range from meters to hundreds of kilometers). The vertical grid consists of 60 layers that use an altitude-based terrain-influenced coordinate system, ranging in thickness from 15 m near the surface to 2.5 km at the top (at a height of ~70km). A nearly unlimited number of multiple-nested, two-way interactive grids may be used in a simulation, allowing the model to resolve small-scale phenomena embedded in larger-scale systems. For example, a three-grid simulation with grid spacings of 80, 40, and 10 kilometers could be used to investigate the large-scale evolution of a baroclinic disturbance (e.g., a low pressure system), while simultaneously allowing the examination of the smaller-scale structure and effects of a frontal zone (e.g., cold front). MRAMS is not a Mars global climate model (MGCM). It has regional, not global coverage, and it is designed to run over relatively short time periods (e.g., five Mars-days). MRAMS therefore requires the user to supply initial conditions and time-dependent boundary conditions, which are routinely obtained from a MGCM solution – we utilize recent NASA Ames Research Center MGCM (Haberle et al., 1993) simulations for these purposes. The time-dependent boundary conditions are needed in order to capture important large-scale atmospheric phenomena (e.g., atmospheric tides

induced by solar heating) that may propagate into and out of the MRAMS domain. Prior related work using MRAMS includes a series of recent simulations targeting Endeavour Crater (where the Mars Exploration Rover Opportunity currently is located), which revealed a topographically-enhanced evening flow regime (~1 Mars-hour in duration, in the southern spring and summer seasons) that correlates with the orientation and movement of the intracrater dunes (Chojnacki et al. 2011). Other flow regimes (at other seasons and times-of-day) were also noted in these simulations, and appear to correlate with other aeolian surface features (Chojnacki et al. 2011).

The set of Gale crater MRAMS simulations analyzed in this work is comprised of four runs at representative seasons ($L_s \sim 30, 120, 210,$ and 300 degrees; each several simulated Mars-days in duration). The surface aerodynamic roughness length (z_0) was set to a constant value (0.03 m) over the MRAMS domain, due to the lack of z_0 spatial distribution data for Mars. The terrain and surface characteristics for these MRAMS simulations were based on $1/128^\circ$ (~460x460 m at the equator) gridded MGS Mars Orbiter Laser Altimeter (MOLA) topography (Smith et al. 2001) and $1/20^\circ$ (~3x3 km at the equator) gridded MGS TES albedo and nighttime thermal inertia (Putzig and Mellon 2007). A total of seven nested grids were used in each of the simulations, with grids 6 and 7 (having grid spacings of ~1.8 km and ~600 m, respectively) being used for the analysis reported here. MRAMS output from the first Mars-day of each run was not analyzed, as model spin-up is still occurring then.

CRISM measurement

Hyperspectral observations from CRISM (Murchie et al., 2007) were used to determine the mineralogy of the dark dunes. Data from the CRISM L (IR, from 1000-3920 nm) detector were collected and used under their most current publicly released calibration version (TRR3). Atmospheric and photometric corrections were implemented using the CRISM Analysis Tool (CAT v7.0) for ENVI (Murchie et al., 2009). Spectra from the dark dunes were ratioed to a spectrally neutral region in the same detector column. This technique suppresses residual artifacts after calibration. CRISM spectra obtained were finally compared with reference spectra present in the CAT spectral library.

References

- Chojnacki, M., D. M. Burr, J. E. Moersch, and T. I. Michaels (2011), Orbital observations of contemporary dune activity in Endeavor crater, Meridiani Planum, Mars, *J. Geophys. Res.*, 116, E00F19, doi:10.1029/2010JE003675.
- Haberle, R. M., J. B. Pollack, J. R. Barnes, R. W. Zurek, C. B. Leovy, J. R. Murphy, J. Schaeffer, and H. Lee (1993), Mars atmospheric dynamics as simulated by the NASA Ames general circulation model, I. The zonal-mean circulation, *J. Geophys. Res.*, 98, 3093– 3123.
- Michaels, T.I., and Rafkin, S.C.R., 2008, Meteorological predictions for candidate 2007 Phoenix Mars Lander sites using the Mars Regional Atmospheric Modeling System (MRAMS): *Journal of Geophysical Research*, 113, E00A07, doi:10.1029/2007JE003013.
- Murchie, S.L., Arvidson, R., Bedini, P., et al., 2007, Compact reconnaissance imaging spectrometer for Mars (CRISM) on Mars Reconnaissance Orbiter (MRO): *Journal of Geophysical Research*, v. 112, E5, E05S03. doi:10.1029/2006JE002682.
- Murchie, S.L., Seelos, F., Hash, C., et al., 2009. The compact reconnaissance imaging spectrometer for Mars investigation and data set from the Mars Reconnaissance Orbiter's primary science phase: *Journal of Geophysical Research*, v. 114, E00D07, doi:10.1029/ 2009JE003344.
- Putzig, N. E., and M. T. Mellon (2007), Apparent thermal inertia and the surface heterogeneity of Mars, *Icarus*, 191, 68-94.
- Rafkin, S.C.R., Haberle, R.M., and Michaels, T.I., 2001, The Mars regional atmospheric modeling system: Model description and selected simulations, *Icarus* 151: 228–256. DOI: 10.1006/icar.2001.6605.
- Smith, D. E., et al. (2001), Mars Orbiter Laser Altimeter: Experiment summary after the first year of global mapping of Mars, *J. Geophys. Res.*, 106, 23689–23722, doi:10.1029/2000JE001364.

Supplemental Figures:

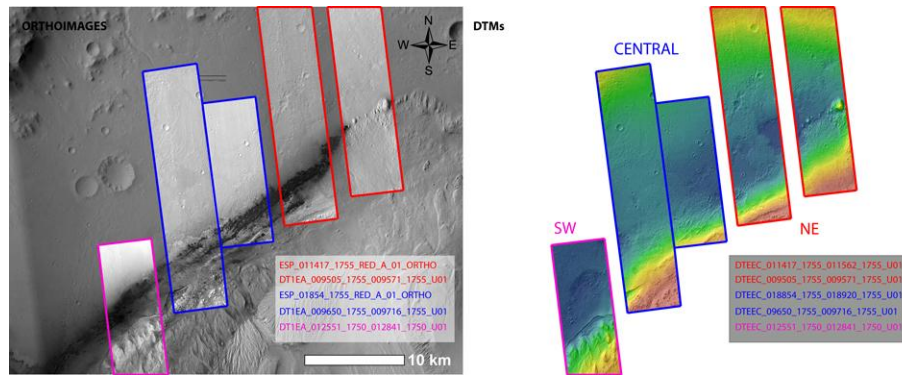


Fig. DR1: List and location of the HIRISE orthoimages and DTMs used in this study. The three stereoplots representing the slipface surface vectors (see main text) have been computed along the dune field in the three sectors highlighted (NE – CENTRAL – SW).

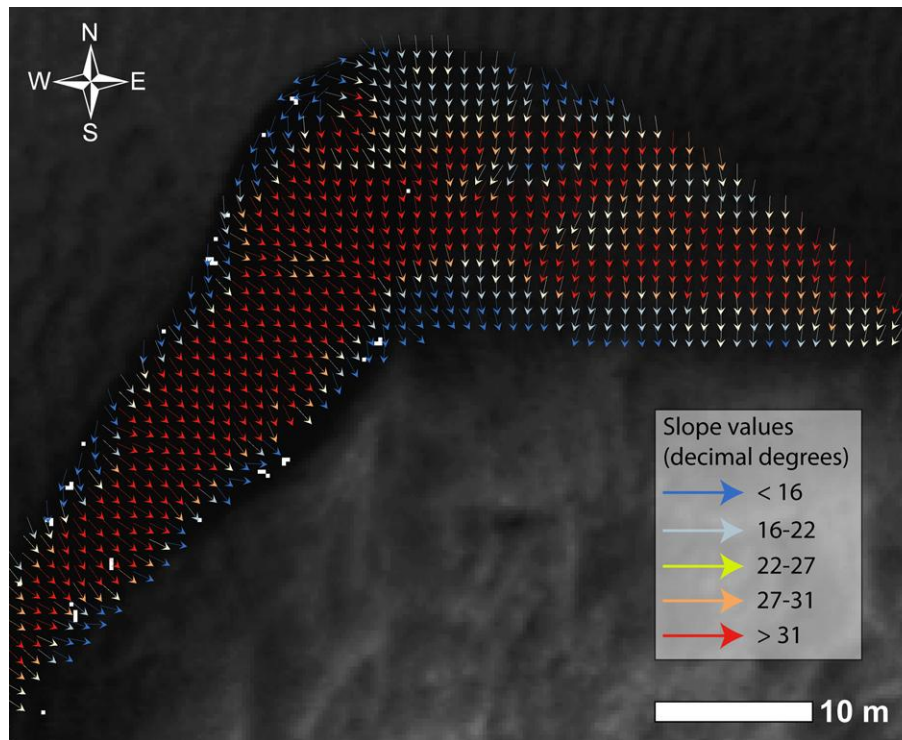


Fig. DR2: Example of the slope vectors computed for the slipface surfaces. The vectors were computed from the DTM and are overlaid on the correspondent HIRISE orthoimage. Those vectors were used to generate the stereonet plots shown in Fig. 1C, which portray the regional trends and dip angles of the splifaces.

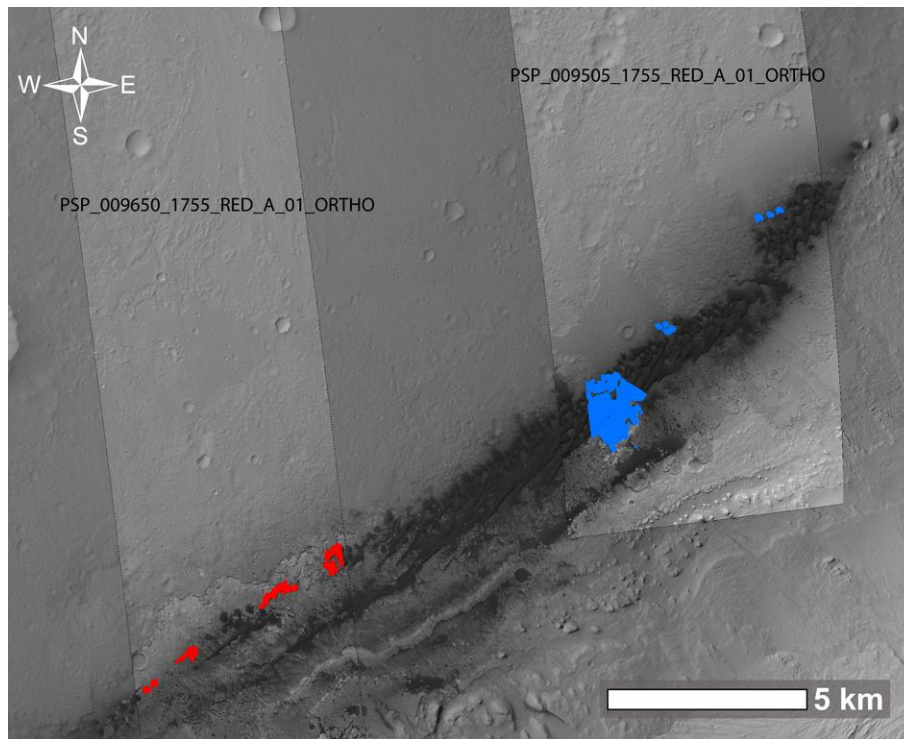


Fig. DR3: Locations where ripple patterns were automatically mapped using two orthorectified HIRISE images with similar illumination conditions (see Table DR1). See Fig. 2 for discussion.

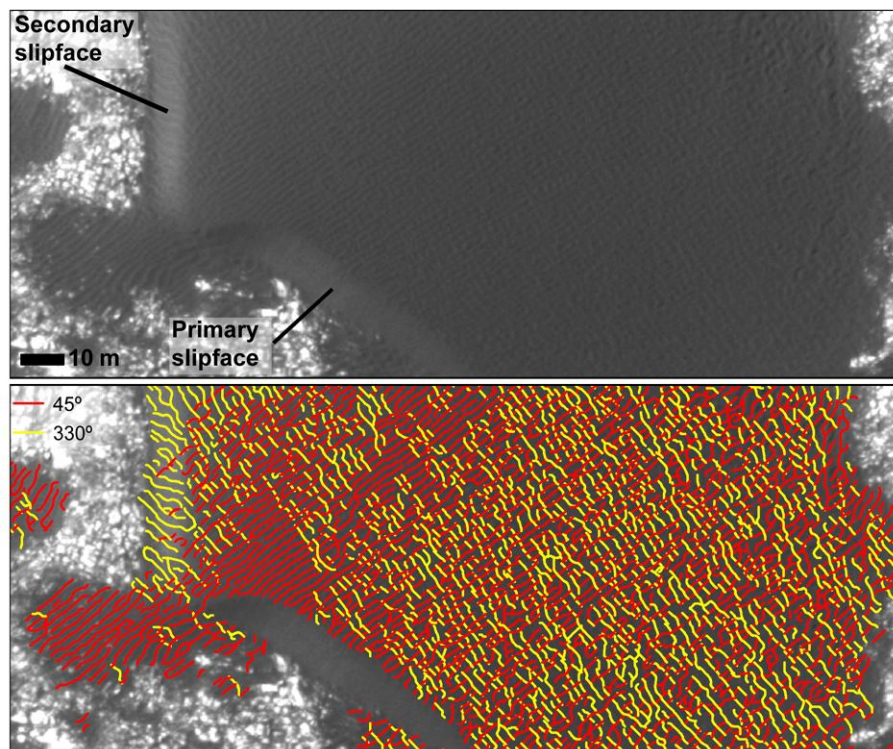


Fig. DR4: Example of the ripples crest lines automatically mapped. In this case, the color code used emphasizes the co-occurrence of two sets of ripples trending 45° and 330° . Note the existence of two distinct slipfaces, with the secondary slipface being reworked by ripples.

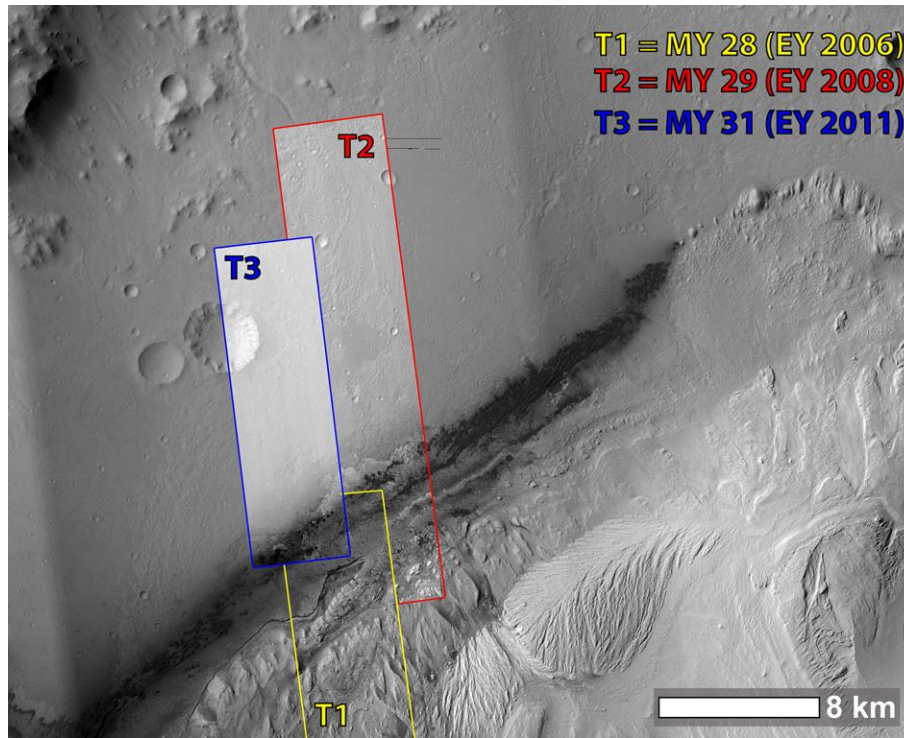


Fig. DR5: List and location of the three orthorectified images used for spatial-temporal change analysis.

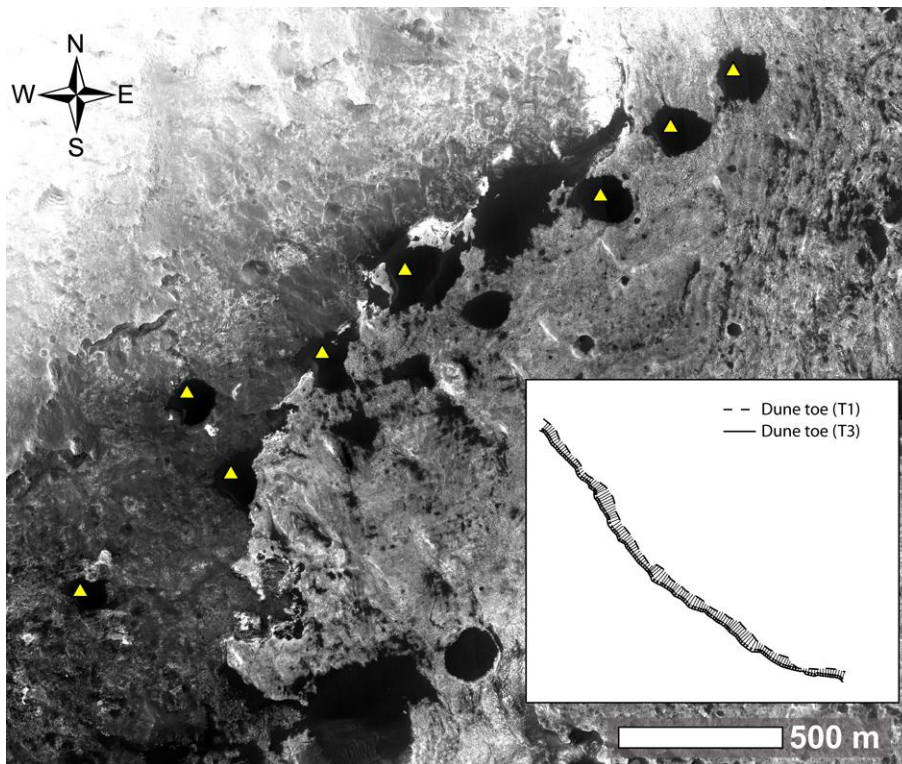


Fig. DR6: Example of the technique used to measure dune migration. We have mapped the dune toe lines at different times and we modeled a bi-orthogonal displacement between the two time-lapse lines. Dune migration was measured over the eight dunes highlighted by the yellow triangles.

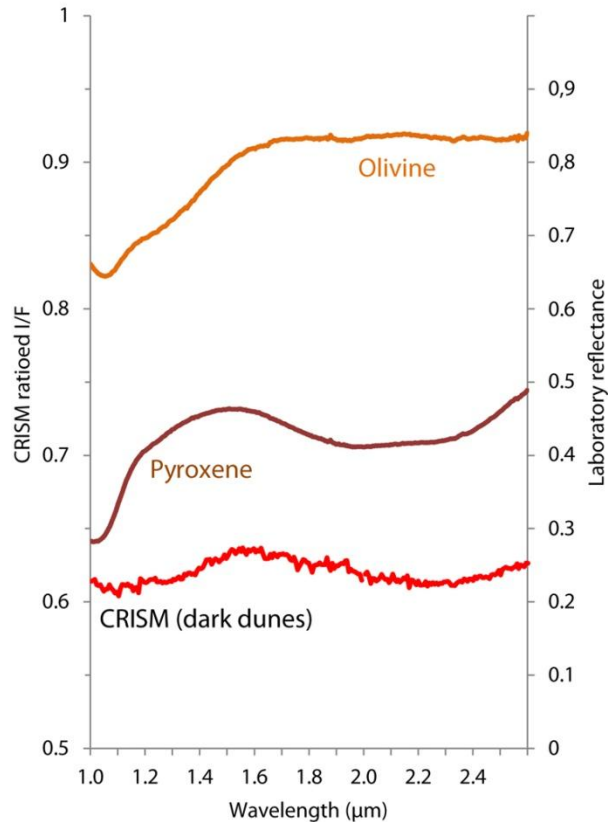


Fig. DR7: ratioed spectra obtained with CRISM for the dark dunes (red spectrum) compared with the best library spectral matches (orange=forsterite, purple=augite).

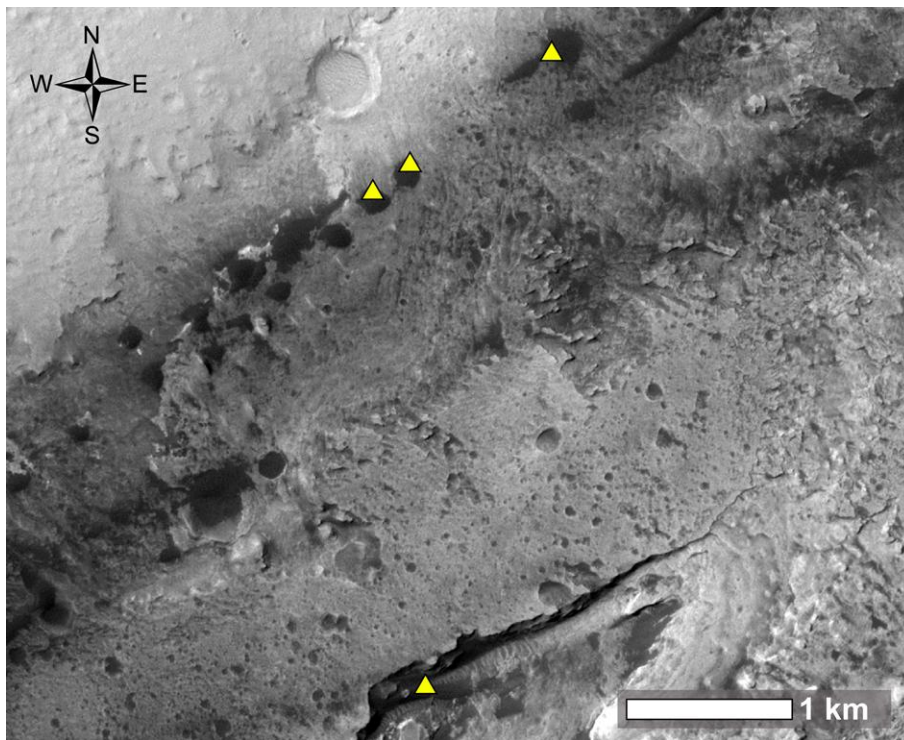


Fig. DR8: ripple migration was computed for 180 ripples over the four dunes highlighted by the yellow triangles.

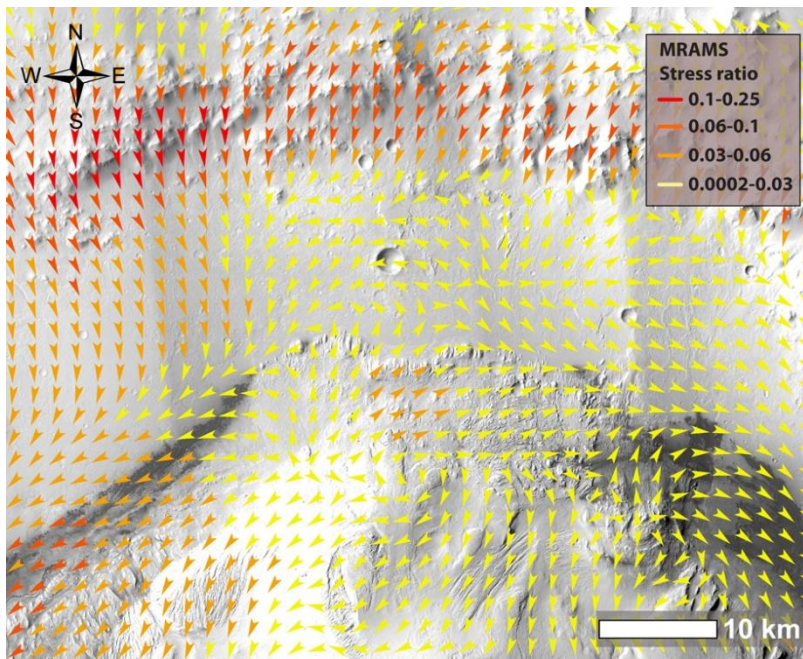


Fig. DR9: Mean stress ratio vectors computed from the MRAMS data (~1.8 km grid spacing). Note the influence of Gale rim and central mound topography.

Supplemental Tables:

	PSP_009505_1755_RED_A_01_ORTHO	PSP_009650_1755_RED_A_01_ORTHO
Source product ID	PSP_009505_1755	PSP_009650_1755
Acquisition date	6 August 2008	17 August 2008
Resolution	0.25 m/pixel	0.25 m/pixel
Latitude (centered)	-4.5 degrees	-4.6 degrees
Longitude (East)	137.5 degrees	137.3 degrees
Local Mars time	3:31 PM	3:26 PM
Solar longitude	108.8 degrees, Northern Summer	113.9 degrees, Northern Summer
Solar incidence angle	59 degrees	57 degrees
Sub solar azimuth	211.3 degrees	210.8 degrees
Emission angle	8.2 degrees	11.6 degrees

Table DR1: Image acquisition parameters of the HiRISE used for mapping the ripple pattern.

	DT1EA_001488_1750_001752_1750_U02 (T1)	DT1EA_009650_1755_009716_1755_U01 (T2)	DT1EA_024234_1755_024300_1755_U01 (T3)
Source product ID	PSP_001488_1750	PSP_009650_1755	ESP_024234_1755
Acquisition date	20 November 2006	17 August 2008	27 September 2011
Resolution	0.25 m/pixel	0.25 m/pixel	0.25 m/pixel
Latitude (centered)	-4.8 degrees	-4.6 degrees	-4.6 degrees
Longitude (East)	137.3 degrees	137.3 degrees	137.2 degrees
Local Mars time	3:31 PM	3:26 PM	2:23 PM
Solar longitude	138.2 degrees, Northern Summer	113.9 degrees, Northern Summer	7.0 degrees, Northern Spring
Solar incidence angle	57 degrees	57 degrees	37 degrees
Sub solar azimuth	203.3 degrees	210.8 degrees	191.3 degrees
Emission angle	2.5 degrees	11.6 degrees	5.8 degrees

Table DR2: T1-T2-T3 HiRISE image acquisition parameters.

Supplemental Animations:

Animation DR1: 330° ripple pattern migration.

Animation DR2: Different migration rates for the 330° and 45° ripple pattern.

Animation DR3: Dune migration in the SW sector of the field between 2006 – 2011 (MY 28-31).

Animation DR4: Dune migration in the SW sector of the field between 2006 – 2011 (MY 28-31).

Animation DR5: Detail of a the migrating dune's toe (MY 28-31).